# Channeling of magnetic flux in $YBa_2Cu_3O_{7-\delta}$ superlattices

**H.J. Mollatt[1], T. Qureishy[1], A. Crisan[2], V.S. Dang[3], P. Mikheenko[1]**

[1]Department of Physics, University of Oslo, P.O.Box 1048, Blindern, 0316, Oslo, Norway

[2]National Institute for Materials Physics Bucharest, 405A Atomistilor Str., 077125,

Magurele, Romania

[3]Nano and Energy Center, VNU Hanoi University of Science, 334 Nguyen Trai, Thanh Xuan, Hanoi, Vietnam

We report unusual effect of channeled magnetic flux motion in $YBa_2Cu_3O_{7-\delta}/PrBa_2Cu_3O_{7-\delta}$ superlattices grown by pulsed laser deposition. Magneto-optical imaging reveals that flux moves along a set of parallel and perpendicular lines, while optical microscopy does not show any features on the surface that may cause this effect. In contrast, scanning electron microscopy registers sub-micron fractures in the superlattices, corresponding to the flux lines, but the magnetic flux channels are much wider than the width of these fractures. To further clarify the origin of flux channels, electrical transport measurements on the superlattices have been performed. Their current-voltage characteristics reveal the presence of distinctive branches related to the flux motion along the selective channels, following which magnetic flux can cross the sample in a shortest and least resistive way. The application of very large current overheated the superlattice along these channels evaporating superconducting material and exposing wider than in the superconductor fractures in the substrate. It is concluded that motion of flux in the channels is controlled not only by the presence of nano-fractures in $YBa_2Cu_3O_{7-\delta}/PrBa_2Cu_3O_{7-\delta}$, but also stresses developed in the superconducting material appearing due to the fracturing of the substrate.

## INTRODUCTION

For practical applications of high-temperature superconductors [1], one of them is $YBa_2Cu_3O_{7-\delta}$ (YBCO), highest possible in-plane critical current density in high magnetic fields should be achieved [2]. This requires the introduction of dense nano-arrays of pinning centers in the material. Related modern techniques for creating these arrays are described in [3]. An efficient way of forming nano-columns that are strong pinning centers for vortices in superconducting films, is to start with deposition of the array of nanoparticles of suitable material on the substrate

before the deposition of the superconducting film. In particular, gold or silver nanoparticles appeared to be very effective for the growth of the nanocolumns of YBCO [4]. Experiments with other, more complicated nanoparticles, proved to be successful as well. In particular, nanoparticles of non-superconducting $PrBa_2Cu_3O_{7-\delta}$ (PBCO) with crystal-lattice parameters that are very close to those in $YBa_2Cu_3O_{7-\delta}$, were found to improve critical current density in the latter material [5]. This effect, however, becomes weaker with larger thickness of YBCO. To overcome this problem, the idea of growing $YBa_2Cu_3O_{7-\delta}/PrBa_2Cu_3O_{7-\delta}$ (YBCO/PBCO) superlattices was suggested with typical thickness of YBCO from tens to hundreds of nanometers and sub-nanometer or nanometer size of PBCO nanoparticles. Such approach allows to grow thick films with good superconducting properties [5,6].

Some YBCO/PBCO superlattices, however, showed low global critical current density, as determined by magnetization measurements. To clarify what is specific about these films, magneto-optical imaging (MOI) was performed on several of them complemented by transport measurements. The results of this investigation are described in this paper.

## EXPERIMENTAL

The YBCO/PBCO superlattices were grown epitaxially by pulsed laser deposition (PLD) on $SrTiO_3$ (STO) substrates. An excimer KrF 248 nm laser with pulse duration of 30 ns was used for the growth. The repetition rate of the laser was 4 Hz, and the distance between the target and substrate, which was kept at 780 °C, was 5.5 cm. The thickness of YBCO and PBCO layers was defined, after the calibration, by the number of laser pulses. Typically 1000 laser pulses results in a thickness of about 250 nm. The following superlattices have been prepared with general formula (PrBCO**n**-YBCO**m**)x**l**, where **n** and **m** are numbers of pulses on PBCO and YBCO targets, respectively, and **l** is number of repetitions of these sequences. Sample A: (PrBCO3-YBCO250)x32; B: (PrBCO3-YBCO250)x48 and C: (PrBCO15-YBCO3000)x4. The superlattices A and B were of about 2 μm and C of about 3 μm thick. In spite of different total thickness, different number of layers and different thickness of individual layers, the superlattices show a common property – well expressed channeling of magnetic flux seen by MOI.

MOI is a technique allowing to visualize distribution of magnetic field in a sample using Faraday rotation [7,8]. As indicator, Bi-substituted iron garnet films have been used [8,9].

Electrical measurements were carried out by a four-contact technique on a rig with power supply, two digital voltmeters and a temperature sensor, all con-

trolled by a MATLAB program. The samples have been cooled by liquid nitrogen or liquid helium. Scanning electron microscopy (SEM) was performed on FEI Quanta 200 FEG-ESEM.

## RESULTS AND DISCUSSION

Figs. 1 to 3 show MOI images of superlattices A to C, respectively. The common feature of the figures is channeled penetration of magnetic flux into the interior of the samples. All three figures contain network of the lines perpendicular to each other. The lines are not directed along the edges of the substrate. The thickness of the lines is similar in all three images, but their density and distribution are different. There are areas in all samples that are free from the lines.

Magnetic flux channeling is quite unusual effect. It cannot be predicted or suggested from magnetization or electrical transport measurements that reflect integral properties of the sample. It emphasizes importance of magneto-optical imaging that gives detailed local information about the sample. The origin of flux lines is not clear, especially taking into account that optical microscopy shows no any line features matching those in Figs. 1- 3.

To clarify nature of lines, SEM was performed on a rectangular area outlined by red line in Fig. 3. The result, together with overlapped MOI image (dark green), is shown in Fig. 4. One can clearly see that in the middle of flux-flow lines, there are sub-micron fractures in YBCO/PBCO, and the magnetic flux penetrates along these fractures. The width of the brightest part of the lines, from which magnetic flux further penetrates into rectangular areas in critical-state fashion [10] is, however, much bigger than width of fractures.

At the increase of magnetic field, magnetic flux starts moving in the sample along the fractures that are closest to the edges of the film, gradually filling bigger areas of superlattice. Some areas, however, remain flux-free. Electrical field and corresponding voltage appears during the change of magnetic configuration in the sample, but when the distribution of magnetic flux is static, as in Figs. 1-4, voltage is absent.

The situation is different when transport current is flowing through the sample in over-critical state. It induces permanent flux flow across the sample. Fig. 5 shows connection of current (red) and potential (green) leads to sample C used to record its current-voltage characteristics. When current is passed through the sample, magnetic flux moves along bright lines of easy flow revealed by MOI in Fig. 5. It is important to note that all bright horizontal lines block vertical flux flow, as it cannot cross dark areas of strong superconductivity in-between. The ‘bottle-

neck' in the current sample is the line below four red arrows in Fig. 5. Only four vertical segments marked by these arrows are available for flux flow. Correspondingly, one could expect four independent branches on current-voltage characteristics. These branches indeed are registered and shown in Fig. 6. Red lines show how transitions between these branches take place.

During flux flow, dissipation of energy takes place mainly along few vertical lines linked to four vertical segments shown by arrows in Fig. 5. At the application of high current, dissipation can be so high that it can evaporate superconducting material. This is exactly what happened with superlattice C.

Fig. 7 shows MOI image of the part of the sample after application of high current that burned the superlattice. This image was obtained by cooling sample in magnetic field of 17 mT to 20 K and then reducing magnetic field to 13.5 mT. Dark lines in the image correspond to areas of evaporated superconducting material. At least three marked vertical segments to the right in Fig. 5 are fully burned during application of high current.

Fig. 8 shows with a higher than in Fig. 7 resolution conventional optical image of a burned channel of superlattice C. It is clearly seen that below evaporated YBCO/PBCO , there is fracture in substrate marked by red arrow in the plot.

All segments of burned lines show presence of fractures in the substrate. It means that these are fractures in the substrate, developed during the deposition, that induce channeling of magnetic flux in the superlattices. The fractures in cubic STO substrate developed along crystallographic directions. The different from 0 and 90º slope of lines in Fig. 1 and Fig. 2 with respect to the edges simply reflects the fact that substrate were cut not exactly along these directions.

In its turn, fractures in substrate induce nano-fractures in PBCO/YBCO and create stresses that weaken superconductivity in rather wide channels that are revealed by MOI. The rectangular array of flux channels is not only a remarkable phenomenon. Being properly controlled, it can find use in practical applications combining strong superconductivity in in rectangular 'windows' and weak, possibly Josephson-like behaviour in nano-fractures in-between.

## SUMMARY

Channeling of magnetic flux along a network of mutually perpendicular lines in $YBa_2Cu_3O_{7-\delta}/PrBa_2Cu_3O_{7-\delta}$ superlattices is reported. A range of experiments have been performed to clarify the nature of this effect. It is found that channels appear due to

fracturing of substrate in the process of pulsed laser deposition and the corresponding stress and nano-fracturing induced in the superconductor. A combination of magneto-optical imaging and electrical transport measurements allows to follow details of flux motion along the network of weak superconducting channels.

## REFERENCES


[1] Marchionini BG, Yamada Y, Martini L, Ohsaki H (2017) High-Temperature Superconductivity: A Roadmap for Electric Power Sector Applications, 2015–2030. IEEE Trans Appl Supercond: 27(4):0500907

[2] Nault RM (ed) (2006) Basic Research Needs for Superconductivity. Report on the Basic Energy Sciences Workshop on Superconductivity, May 8-11, 2006, Argonne National Laboratory, Arlington

[3] Crisan A, Dang VS, Mikheenko P (2017) Nano-engineered pinning centres in YBCO superconducting films. Physica C 553:118-132

[4] Mikheenko P, Sarkar A, Dang VS, Tanner JL, Abell JS, Crisan A (2009) c-Axis correlated extended defects and critical current in $YBa_2Cu_3O_x$ films grown on Au and Ag-nano dot decorated substrates. Physica C 469(14):798–804

[5] Crisan A, Dang VS, Mikheenko P, Tse YY, Sarkar A, Bowen J, Abell JS (2009) Pinning potential in thick $PrBa_2Cu_3O_y/YBa_2Cu_3O_x$ quasi-multilayers. Physica. C 470(1):55-60

[6] Dang VS, Mikheenko P, Sarkar A, Abell JS, Crisan A (2010) Critical current density in $Ag/YBa_2Cu_3O_x$ and $PrBa_2Cu_3O_y/YBa_2Cu_3O_x$ multilayers. Journal of Physics: Conference Series 234(1):012010

[7] Johansen TH, Shantsev DV (eds) (2004) Magneto-Optical Imaging. Kluwer Academic Publishers, Dordrecht

[8] Jooss Ch, Albrecht J, Kuhn H, Leonhardt S, Kronmüller H (2002) Magneto-optical studies of current distributions in high-Tc superconductors. Rep Prog Phys 65(5):651–788

[9] Mikheenko P, Yurchenko VV, Cardwell DA, Shi YH, Johansen TH (2013) Magneto-Optical Imaging of Superconductors for Liquid Hydrogen Applications. Journal of superconductivity and novel magnetism 26(5):1499-1502

[10] Mikheenko PN, Kuzovlev YuE (1993) Inductance measurements of HTSC films with high critical currents. Physica C 204(3-4):229-236


Figure 1: Magnetic flux pattern in superlattice A composed of 32 YBCO layers. The temperature of the sample is 3.7 K. A magnetic field of 60 mT was applied after cooling sample in zero magnetic field.


Figure 2: Magnetic flux pattern in superlattice B composed of 48 YBCO layers. The temperature of the sample at the record is 3.7 K. A magnetic field of 60 mT was applied after cooling sample in zero magnetic field.

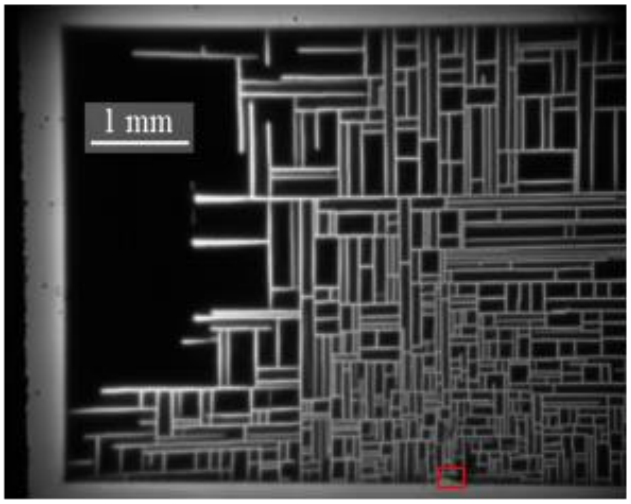


Figure 3: Magnetic flux penetration into superlattice C composed of 4 layers of YBCO. The temperature of the record is 20 K. A magnetic field of 34 mT was applied after cooling sample in zero magnetic field.

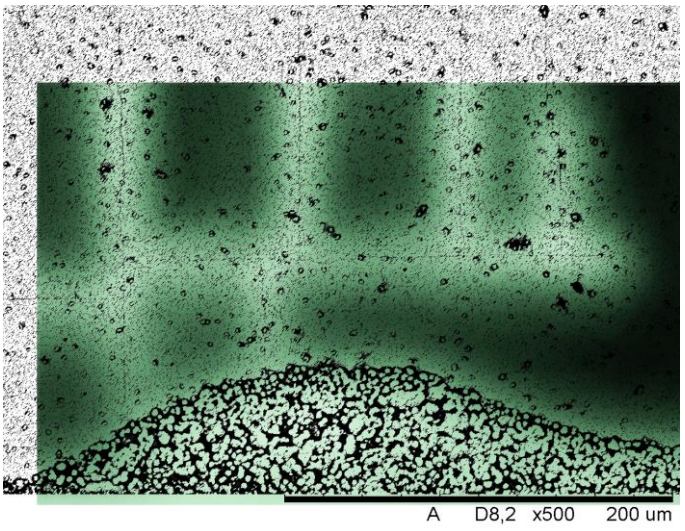


Figure 4: Scanning electron microscopy image of the rectangular area outlined by red line in Fig. 3 with overlapped MOI image (dark green). Sub-micron fractures are seen along the lines of the accumulation of magnetic flux.

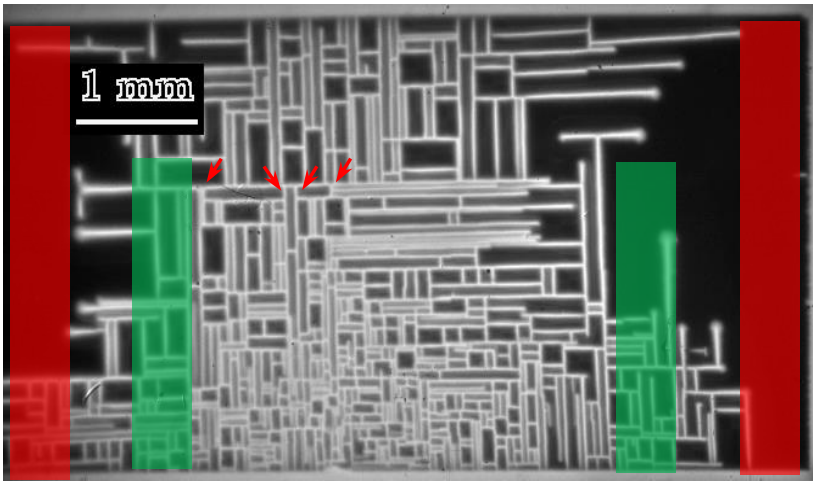


Figure 5: Position of current (red) and potential (green) leads at the record of current-voltage characteristics of the superlattice C.

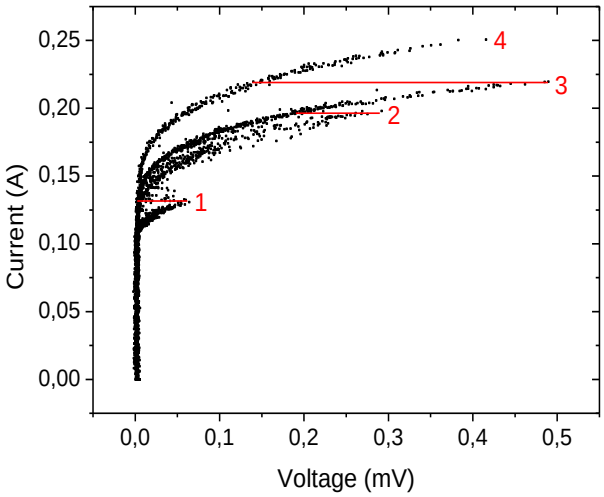


Figure 6: Current-voltage characteristic of the superlattice C with current and potential leads as in Fig. 5. Four branches of characteristic corresponding to vertical segments marked by red arrows in Fig. 5 are seen in the plot. Red lines show how transitions between different states take place.

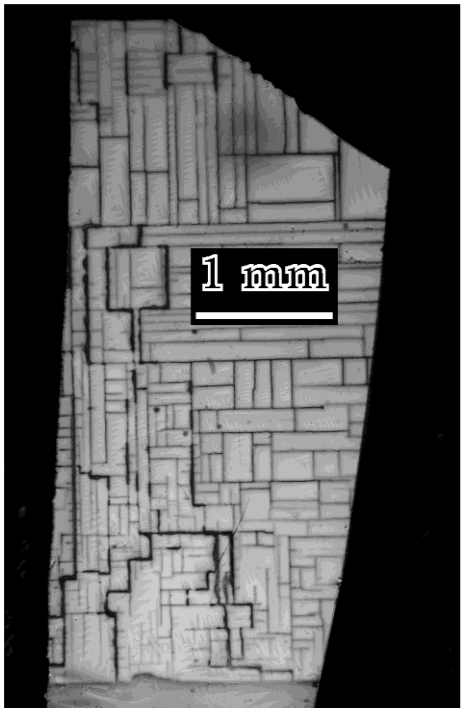


Figure 7: MOI image of the part of the superlattice C after application of high current that burned the sample. This image is obtained by cooling sample in magnetic field of 17 mT to 20 K and then reducing magnetic field to 13.5 mT. Dark lines correspond to areas of evaporated superconducting material.

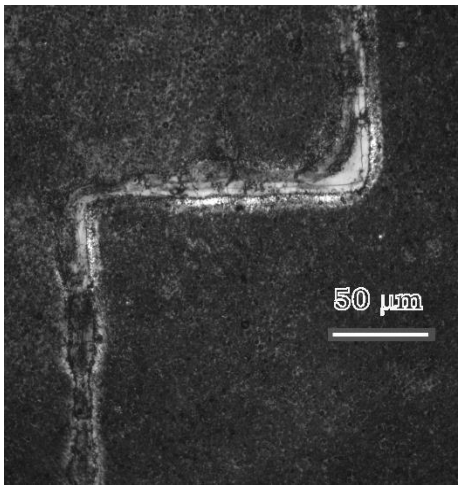


Figure 8: Conventional optical image of a burned channel of the superlattice C.